RSC Advances

ROYAL SOCIETY OF CHEMISTRY

www.rsc.org/advances

Supramolecular complexes involving non-symmetric viologen cations and hexacyanoferrate(II) anions. A spectroscopic, crystallographic and computational study

Raffaello Papadakis,[a,b]* Ioanna Deligkiozi,[b] Michel Giorgi,[c]

Bruno Faure,[d] and Athanase Tsolomitis[b]

[a] *Department of Chemistry (BMC) Uppsala University, Box 576 751 23 Uppsala, Sweden;* [b] *School of Chemical Engineering, Laboratory of Organic Chemistry, National Technical University of Athens, 15780 Athens, Greece;* [c] *Aix-Marseille Université, CNRS FR1739, Campus St. Jérôme, Spectropole, 13013 Marseille, France;* [d] *Aix Marseille Université, CNRS, Centrale Marseille, ISM2 UMR 7313, 13397, Marseille, France.*

Abstract:

We have investigated spectrally, crystallographically as well as computationally the charge transfer complexes of newly synthesized N-aryl-N′-methyl non-symmetric viologens (AMVs) with hexacyanoferrate(II) (HCF) anions. The supramolecular binding of AMVs and HCF was studied in solution and in the crystal state for one of the obtained complexes. Substituent effects on the electron affinities of the dicationic AMVs, determined using Mulliken's theory [R. S. Mulliken, *J. Am. Chem. Soc.*, 1952, **14**, 811-824] were quantified. The structure of one of the AMV//$Fe^{II}(CN)_6$ pairs solved through Single-Crystal X-ray Diffraction (SCXRD), provided insights for the supramolecular binding of the anionic and cationic counterparts and the role of lattice water molecules. Supramolecular binding in solution, studied with the use of NMR spectroscopy, is in agreement with the results obtained in the solid state.

Introduction:

Viologens are a well-known family of heterocyclic compounds with numerous applications in various research areas.[1] Their strong electron accepting aptitude along with their ability to undergo one-electron reversible reductions, both chemically and electrochemically, giving relatively stable intensely colored radical-cations, has attracted much interest for uses in printing and displaying technologies.[2,3] Additionally 4,4′-bipyridines can serve as building blocks in photoactive molecular shuttles,[4] electrochromic devices,[3,5] biochemical sensors,[6-7] small viologen-based medium responsive molecules,[8] *monoquat*-ligated pentacyanoferrate(II) solvatochromic complexes[9,10,11,12] as well as important components in photoconductive interlocked molecules.[13] The use of viologen halide salts in photochromic applications has also attracted much interest.[14] Charge transfer is a very important feature for the aforementioned photochemical activity of viologens, and it can also occur between the organic counterparts in viologen/electron donors charge transfer complexes.[15,16,17] Utilization of hexacyanoferrate(II) anions and 4,4′-dipyridinium dications to build charge transfer complexes (CTCs) has attracted much attention as well. The first CTCs of that type were reported as early as 1963 by Nakahara and Wang, bearing the symmetric methylviologen[18] (also known as *paraquat*). Ever since several studies in solution[19,20,21] as well as some crystallographic studies were reported.[22,23,24] Noteworthy, the number of crystallographically analyzed CTCs with charged N-heterocycles remains small up to date. The interionic charge transfer (IICT) of the viologen/hexacyanoferrate(II) CTCs resembles the intervalence charge transfer (IVCT) of Prussian blue, responsible for its characteristic deep blue color. IICT between the $[Fe^{II}(CN)_6]^{4-}$ electron rich and the viologen (electron deficient) counterparts is of great interest in these complexes. The electronic spectra of such viologen based CTCs can be readily affected by

different factors, such as pressure,[25] temperature,[24,26] and light[14,27] therefore opening new routes towards novel chromic systems. Hitherto, a big number of CTCs bearing variously substituted dipyridinium salts, such as various paraquats[14-27] lucigenin,[28] and several diquats (diquaternized 2,2′-bipyridinium salts)[29] acting as the electron deficient (cationic) parts of these CTCs, have been reported. However, to the best of our knowledge only CTCs containing symmetric viologens have been reported up to now. In this work we report the synthesis, study in-solution as well as crystallographic study of new CTCs of hexacyanoferrate(II) and non-symmetric viologens. The effect of different substituents on the two nitrogen atoms of 4,4′-bipyridine on the ^{1}H-NMR and UV-Vis spectra of these new CTCs obtained in solution, in combination with the data collected crystallographically, are used in order to rationalize the structure-properties relation.

Results and Discussion

Synthesis and Characterization

In this work a group of six non-symmetric viologens (N-aryl-N′-methyl **v**iologens: AMVs) were synthesized and fully characterized using various spectroscopic techniques. The general synthetic route followed for the synthesis of viologens **4** and **6a-e** is depicted in Scheme 1. The "monoquat" precursor **1** which was synthesized according to a previously described method,[10] gave through quaternization of the second N atom, *via* a reaction with MeI, product **2** in high yield. The latter compound was purified through two sequential anion exchanges yielding the viologen **4** as a dichloride salt. This compound was further used both for the study of its supramolecular complexation with $Fe^{II}(CN)_6$, as well as for the synthesis of the group of AMVs **6a-e**. The latter were prepared through Zincke reactions of **4** with suitable anilines in MeOH.

The reaction times significantly depended on the aryl substituent varying within 4-96 h, and the AMVs in all cases were isolated in yields higher than 68 %.

Compounds **4** and **6a-e** were preferably isolated as dichloride salts, because of their higher solubility in water as compared to the mixed Cl^-, I^-salts. Solubility in water is very important for the formation of the AMVs // $Fe^{II}(CN)_6$ ion pairs.

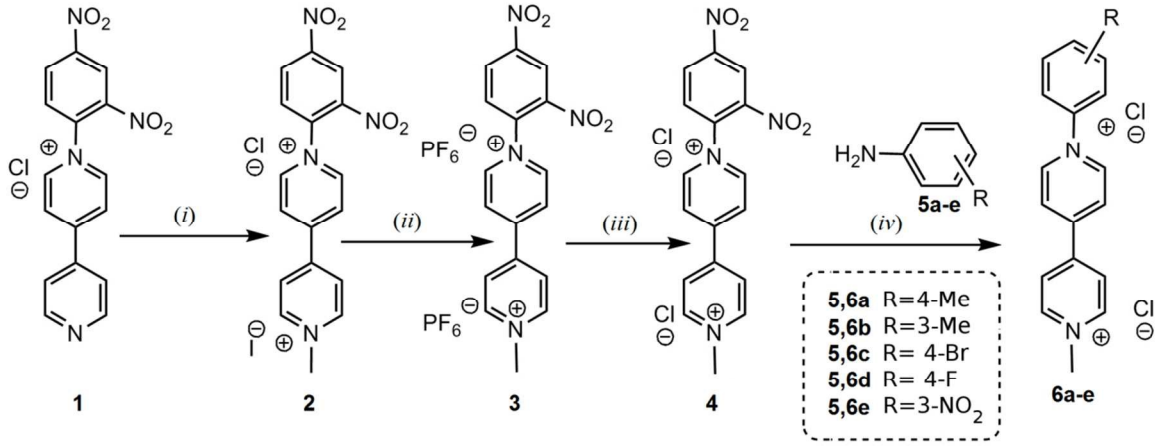

Scheme 1. Synthetic route followed for the preparation of viologens **4** and **6a-e**. (*i*) Δ, MeI in EtOH (*ii*) Δ, aqueous NH_4PF_6. (*iii*) Excess of $Et_4N^+Cl^-$ in MeCN. (*iv*) Zincke reaction. Refluxing MeOH,− 2,4-dinitraniline.

The AMVs were characterized using standard analytical methods including ^1H and ^{13}C NMR spectrposcopy, electrospray high resolution mass spectrometry (ESI HRMS) as well as UV-Vis specrtrophotometry. The ESI HRMS of all AMV chloride salts (**4** and **6a-e**) exhibited peaks corresponding to the radical cations : $AMV^{+\bullet}$ (See supplementary data file). All measured m/z of [AMV-2Cl^-] radical cation species are listed in the experimental section.

On the structure of CTCs

Mulliken's theory accounts CTCs as resonance hybrids of non-polar and dative structures. Assuming the chemical equation of Scheme 2 in case of a CTC between an electron acceptor (A) and an electron donor (D) and Ψ_0 and Ψ_1 the wave functions describing the non-polar (D---A) and dative (D^+---A^-) resonance structures respectively, the wave functions describing the CTC in its electronic ground and excited state (Ψ_G and Ψ_E respectively) will be given by the equations shown in Scheme 2. Absorption of light and photoexcitation of the CTC facilitates the charge transfer from D to A, consequently rendering the dative resonance structure more important than the non-polar resonance structure in the excited state. The opposite applies to the electronic ground state. In other words in the electronic ground state it will be: $|a| > |b|$ whereas in the excited state $|a^*| < |b^*|$, where a and a^* correspond to the coefficients of the wave function Ψ_0 in the ground and excited state respectively whereas b and b^* correspond to the coefficients of the wave function Ψ_1 in the ground and excited state respectively (Scheme 2).

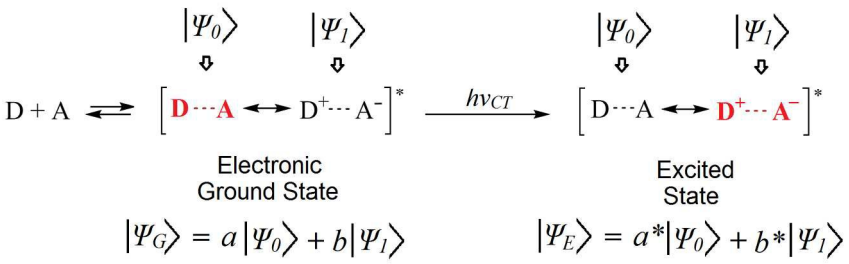

Scheme 2.

From the many theories on CTCs, Mulliken's theory is probably the most applicable in a wide range of CTCs.[30,31] This theory provides a relation of the charge transfer energy (E_{CT}) of a CTC with the electron affinity of the electron withdrawing part (E_A) and the ionization potential of the electron donating part (I_D) of the CTC, according to the following equation:

$$E_{CT} = I_D - E_A + \Delta$$

In this equation Δ corresponds to the difference between the sum of van der Waals, exchange, repulsion, as well as CT resonance energies, and the excited and ground states of the charge transferred.

Formation of the CTCs in solution

The formation of a CTC of the type AMV//$Fe^{II}(CN)_6$ is typically followed by intense coloration (green to blue). Even though aqueous solutions of an AMV salt and $K_4Fe^{II}(CN)_6$ are colorless, upon mixing these two solutions, a deep colored solution is obtained. The appearance of weak visible bands in the electronic spectra of aqueous equimolar mixtures of AMV and $Fe^{II}(CN)_6$ is attributed to the transition: $d(t_{2g}^6).p(\pi^0)^* \rightarrow d(t_{2g}^5).p(\pi^1)^*$. As shown in Figure 1 the energy of the aforementioned transition (E_{CT}) in water is highly affected by the electron donating or withdrawing nature of the phenyl substituent of the AMVs. A bathochromic shift of the charge transfer visible band maximum, of approx. 60 nm (ΔE_{CT} = 0.207 eV) was observed when going from the electron donating group (*m*-tolyl) to the strong electron accepting substituent DNPh (Table 1). This variation of the charge transfer energy is clearly connected to the tunable electron accepting ability of the AMVs which is strongly dependent on the nature of the phenyl substituent. Benniston *et al.*[32] have recently indicated the importance of the torsion angles around the pyridinium rings of some viologens. Herein, focus will be placed on the substituent effects, which are according to our spectroscopic results the most dominant. As anticipated, increasing the electron accepting character of the aforementioned substituent renders viologen dications more prone to reduction by hexacyanoferrate(II) anions (see ESI different resonance structures for DNPh). The Hammett plots of the charge transfer energies (E_{CT}) depicted in Figure 2 shows a very good correlation between E_{CT} and σ. A ρ value of −0.115 (±0.028) eV is obtained through

linear regression. The negative ρ value reflects the bathochromic effect observed while increasing the electron withdrawing character of the aryl substituent of the AMVs.

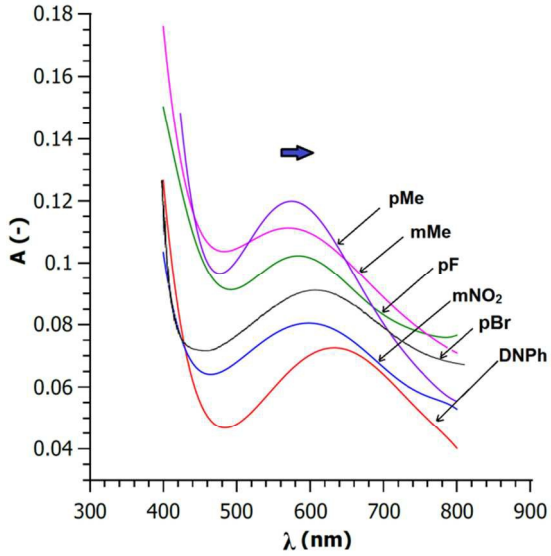

Figure 1. The visible charge transfer band observed in aqueous solutions of **4,6a-e** containing $[Fe^{II}(CN)_6]^{4-}$ at equal concentrations (10 mM). Blue arrow indicates bathochromism while going from electron donating to electron withdrawing substituents.

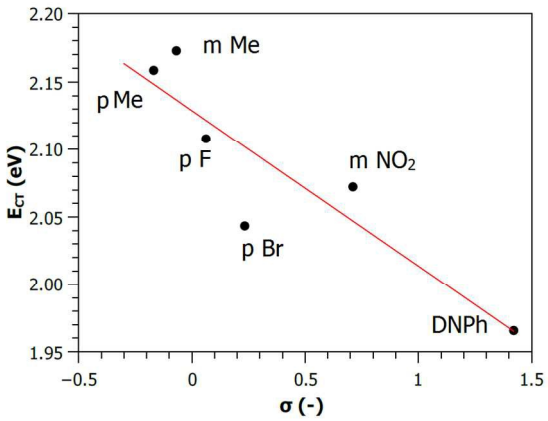

Figure 2. Hammett plot of the experimentally determined charge transfer energies (E_{CT}) of the CTCs between the viologen cations **4**,**6a-e** (AMVs) and hexacyanoferrate(II) anions. E_{CT} were determined in

water solutions at 25 °C with [AMV] = [$Fe^{II}CN_6$] = 10 mM. Relation obtained through linear regression: $E_{CT} = -0.115\ (\pm 0.028)\sigma + 2.129\ (\pm 0.018)$; R = 0.900.

In addition to the emergence of the characteristic visible IICT band upon mixing AMVs with $Fe^{II}(CN)_6$ anions in water, significant changes in the ^{1}H-NMR spectra of AMVs are also observed upon complexation. This effect was first reported by Haque, Coshow and Johnson, who noticed that because of the electrostatic interactions between the methylviologen dications and the $Fe^{II}(CN)_6$ anions in solution, significant down-field shifts were observed on the proton signals of the aromatic rings of 4,4′-bipyridyl.[33] As long as these interactions are electrostatic, they should be drastically affected by the distance between anions and cations. Hence, for a symmetric viologen cation (such as methylviologen) there should be an equal electrostatic effect on both pyridine rings of 4,4′-bipyridyl. However, for non-symmetric viologens (e.g. the AMVs studied in this work) the effect of the $Fe^{II}(CN)_6$ anions on the two rings 4,4′-bipyridyl, is expected to be different, due to different charge distribution along the 4,4′-bipyridyl backbone. Consequently, ^{1}H-NMR spectroscopy becomes an important tool for understanding the local effect of the ion pairing between the AMV cations and $Fe^{II}(CN)_6$ anions in solution. (Dependence of Δδ on Hammett parameter can be found in Supplementary Information)

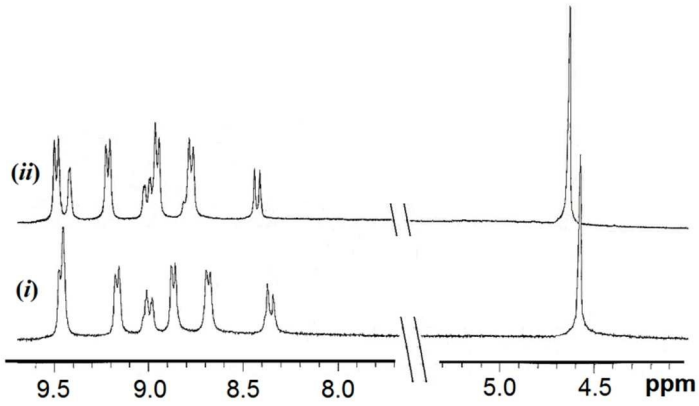

Figure 3. ^{1}H-NMR spectra of (*i*) **4** in D_2O and (*ii*) of the CTC: **4**//$Fe^{II}(CN)_6$ formed in D_2O at 25 °C; [$\mathbf{4}^{2+}$] = [$(Fe^{II}(CN)_6)^{4-}$] = 38 mM.

As listed in Table 1, the extent of down-field shifts of the proton signals (both aromatic and methyl protons) induced upon mixing AMV chlorides with $K_4Fe^{II}(CN)_6$ in equimolar quantities in D_2O strongly depends on the nature of the group attached to the aryl substituents of the AMVs. For the CTC $\mathbf{4}^{2+}$// $Fe^{II}(CN)_6$ for instance, all proton signals are down-field shifted when compared to the ones obtained for the dichloride salt of $\mathbf{4}^{2+}$ (Figure 4).

Table 1. Chemical shifts observed for the AMVs **4**,**6a-e** when codissolved in D_2O with $K_4[Fe(CN)_6]$ in equimolar quantities (assignment of protons according to Fig. 4).

Compound	$\Delta\delta_a$ (ppm)†	$\Delta\delta_b$ (ppm)†	$\Delta\delta_c$ (ppm)†	$\Delta\delta_d$ (ppm)†	$\Delta\delta_{Me*}$ (ppm)†
6a	0.027	0.099	0.135	0.135	0.069
6b	0.037	0.088	0.126	0.130	0.054
6c	0.040	0.083	0.122	0.122	0.047
6d	0.042	0.072	0.121	0.120	0.038
6e	0.051	0.086	0.143	0.141	0.045
4	0.078	0.067	0.183	0.153	0.061

† $\Delta\delta$ are determined as the difference: ($\delta_{AMV//FC} - \delta_{AMV}$) where $\delta_{AMV//FC}$ corresponds to the chemical shift of a certain type of protons of AMV^{2+} in the presence of $[Fe^{II}(CN)_6]^{4-}$ and δ_{AMV} corresponds to the chemical shift of the same type of protons of the AMV^{2+} cation with counter anion Cl^-. All measurements were performed in D_2O at 25 °C. For the determination of δ_{AMV}: [$AMVCl_2$] = 38 mM and for $\delta_{AMV//FC}$ [$AMVCl_2$] = [$K_4[Fe(CN)_6]$] = 38 mM.

*$\Delta\delta_{Me}$ corresponds to the $\Delta\delta$ of the Me protons attached directly to a nitrogen atom of an AMV.

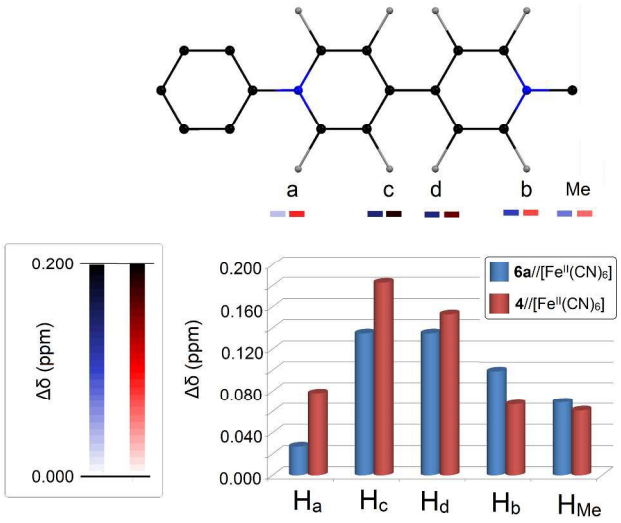

Figure 4. Histogram showing the ^{1}H-NMR shifts (Δδ) for **4** and **6a**, after mixing these AMVs with $K_4[Fe(CN)_6]$ in equimolar quantities ([AMV] = $[K_4[Fe(CN)_6]]$ = 38 mM) in D_2O at 25 °C. (Δδ values for all AMVs are listed in table 1). Insets: assignment of 4,4′-bipyridine protons used in this work (top) and color-scale of Δδ (left); the darker the colour, the higher the Δδ observed.

Determination of Electron affinities for 4 and 6a-e.

According to the theory of Mulliken describing CTCs it is also possible to determine the E_A of the AMVs. Equation 1 connects E_A and E_{CT}. In this equation using the value of I_D = 3.50 eV obtained by Monk and coworkers[34] and letting only E_A vary, it is possible to calculate E_A according to a previously described methodology.[31,34] The values of E_A obtained for the AMVs through that procedure are listed in Table 2. The characteristic equation E_{CT} *vs* E_A obtained for the CTCs of AMVs with ferrocyanide(II) anions, is the following:

$$E_{CT}\,(\text{eV}) = -\,[0.956\ (\pm 0.161)]\,E_A + 3.604\ (\pm 0.256)\,;\ \text{R} = 0.947;\ \text{RSS} = 0.003$$

This characteristic equation for ferrocyanide(II) anions connects the charge transfer energy which is the energy needed for an electron to be transferred from the iron(II) center to an electron deficient AMV dication with the electron affinity of the AMV. The negative slope

obtained indicates that the charge transfer becomes more favorable when going to viologens with higher electron affinity, as anticipated.

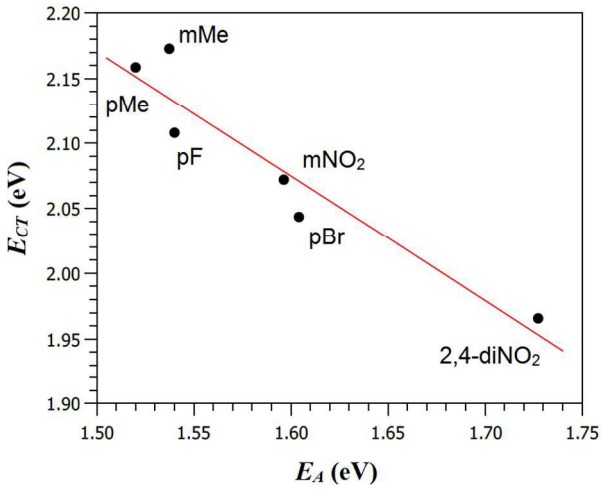

Figure 5. Plot of the experimentally determined charge transfer energies *vs* the electron affinities of the AMVs as determined through Mulliken's theory.

We have further validated our results by extrapolation of the obtained linear relation (E_A *vs* E_{CT}) to methylviologen. The CTC of the aforementioned symmetric viologen with hexacyanoferrate(II) exhibits an E_{CT} value of 2.36 eV (525 nm).[34] Thus the value E_A = 1.35 eV is obtained for methylviologen which is in good agreement with the reported value 1.24 eV by White.[35,34] As anticipated the electron affinity of methylviologen is significantly lower than the obtained E_A values of the AMVs studied in this work, apparently as a result of the electron withdrawing character of the substituted phenyl group on one of the two quaternized nitrogens of AMVs. Even with electron donating substituents such as *p*Me on the phenyl ring (the case of AMV **6a**) the electron affinity of the AMV (~1.52 eV) is approx. 23% higher than that for methylviologen determined by White.[35]

Moreover, E_A strongly depends on the electron donating or accepting nature of the aryl substituent (ρ = 0.121±0.018 eV; R = 0.957. Plot is found in Supplementary Information).

Table 2. Charge transfer energies (E_{CT}) and maxima charge transfer wavelengths (λ_{max}) for CTCs between the **4,6a-e** cations and $[Fe^{II}(CN)_6]^{4-}$ along with electron affinities (E_A), calculated LUMO energies (E_{LUMO}) and HOMO-LUMO energy gaps (E_{GAP}) of **4** and **6a-e**.

Viologen	Substituent	σ_x	λ_{max} (nm)[b]	E_{CT} (eV)[c]	E_A (eV)[d]	E_{LUMO} (eV)[e]	E_{GAP}(eV)[f]
6a	4-Me	-0.170	574.4	2.158(5)	1.519(9)	-3.805(8)	3.671(1)
6b	3-Me	-0.069[a]	570.6	2.172(8)	1.537(3)	-3.821(3)	3.650(7)
6c	4-F	0.062	588.1	2.108(2)	1.539(9)	-3.846(6)	3.854(5)
6d	4-Br	0.232	606.7	2.043(6)	1.604(0)	-3.910(5)	3.544(8)
6e	3-NO_2	0.710[a]	598.3	2.072(3)	1.596(2)	-3.937(8)	4.381(3)
4	2,4-DiNO_2	1.420[a]	630.7	1.965(8)	1.727(2)	-3.942(4)	4.853(4)

[a] For **6b** and **6e** the σ_m values were used. For **4**, the σ value 1.420 corresponds to the $\Sigma(\sigma_p(NO_2))$.

[b] Determined from the first derivatives of Gaussian fitted curves.

[c] $d(t_{2g}^6).p(\pi^0)^* \rightarrow d(t_{2g}^5).p(\pi^1)^*$ transition energies.

[d] Determination of E_A of **4** and **6a-e** was based on Mulliken's theory on charge transfer complexes.

[e] PCM(H_2O)-B3LYP 6-311G(d,p) calculated LUMO energies (for details see Supplementary Information).

[f] HOMO-LUMO gap based on the calculated HOMO and LUMO energies of 4 and 6a-e by PCM(H_2O)-B3LYP 6-311G(d,p) (for details see Supplementary Information).

We furthermore calculated the LUMO and HOMO energies for the dications of the viologens **4**, **6a-e** within Density Functional Theory (DFT). DFT is a very convenient computational tool which has recently been employed in case of viologen/iodide ion pairs, resulting in a very good agreement between experiments and computations.[36] Herein we have calculated the LUMO and

HOMO energies for all AMV-dications, employing functionals including dispersion effects (see computational details section as well as the Supplementary Information) and we have found that E_A correlates very well with the calculated LUMO energies (Figure 6A).[37] E_{LUMO} can serve as a good measure of the electron accepting aptitude of a viologen, reflecting its propensity to undergo one-electron reductions. For the viologens studied here, the electron accepting aptitude follows the sequence **4** > **6e** > **6d**> **6c**> **6b**> **6a** (see Table 2 and Figure 7) and varies linearly with the Hammett parameter σ (see the Supplementary Information).

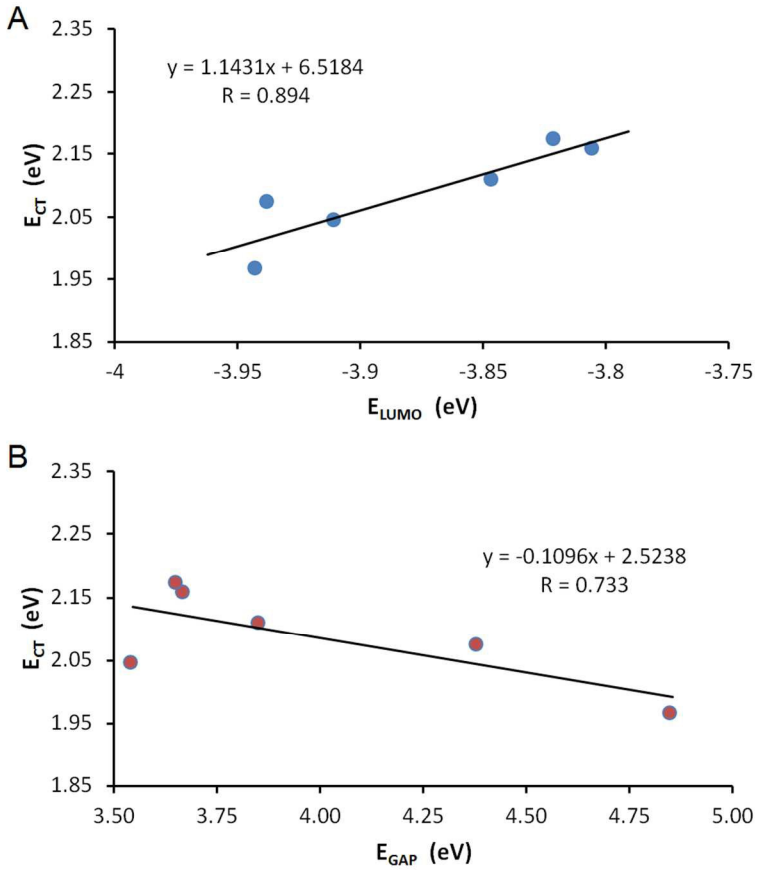

Figure 6. Plots showing the linear correlation of the charge transfer energies of **4** and **6a-e** with (A) the B3LYP 6-311G(d,p) LUMO energies and (B) the calculated HOMO-LUMO energy gap for **4** and **6a-e** at B3LYP 6-311G(d,p).

We have furthermore observed a good correlation between the calculated HOMO-LUMO energy gaps (E_{GAP}) and the electron affinities of **4** and **6a-e** (see Figure 6B). E_{GAP} reflects the inherent capacity of a compound to undergo intramolecular charge transfer. In case of the viologens studied here, it further indicates that intramolecular charge transfer would be energetically more feasible with electron donating substituents on the phenyl ring attached to one of the quaternized nitrogen atoms of the viologen. The tunable character of E_{GAP} is reflected by the very good correlation of the calculated E_{GAP} with the Hammett σ parameter (see Supplementary Information). Now, an increased intramolecular CT aptitude should be connected to a decreased intermolecular CT capacity as long as it is associated with the reduced electron accepting character for the 4,4′-bipyridine backbone (the latter is more electron rich when electron donor substituents are present). This is why a negative slope is obtained for the linear correlation E_{CT} *vs* E_{GAP} (Figure 6B).

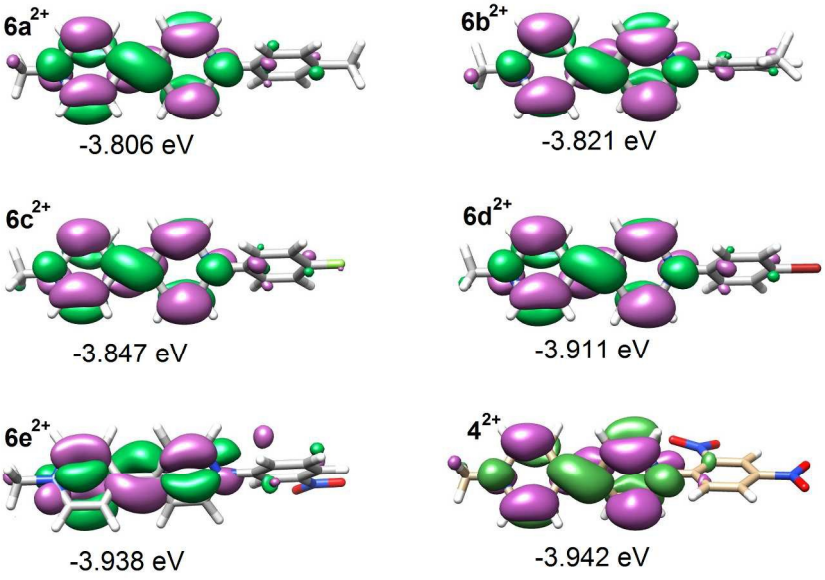

Figure 7. Representations of LUMOs for the dications of the viologens **4** and **6a-e** calculated at PCM(H_2O)-B3LYP 6-311G(d,p).

Crystal structure of complex 7

The CTC **7** was formed in water by mixing (**6a**$^{2+}$)Cl_2 and $K_4Fe^{II}(CN)_6$ (see experimental details). **7** was self-precipitated shortly after mixing the solutions of **6a**$^{2+}$ and $[Fe^{II}(CN)_6]^{4-}$ as a greenish-blue powder, sparingly soluble in cool water but soluble in warm water and several polar organic solvents (e.g. DMSO). **7** was thus recrystallized from water by heating an aqueous suspension of the obtained green powder of **7** (not exceeding 70^{o} C). When **7** is fully dissolved in water, the resulted solution has a deep blue coloration. After letting the solution slowly cool down to r.t. rhombic crystals of **7** were formed which were suitable for SCXRD (Figure 8). Unfortunately, in our hands the rest of the ion pairs of **4** and **6b-e** with $[Fe^{II}(CN)_6]^{4-}$ formed in-solution did not give crystals. Especially the CTC **4**$^{2+}$//$Fe^{II}(CN)_6$ was surprisingly soluble in cool water, presumably because of the hydrogen bonding interactions with water molecules.

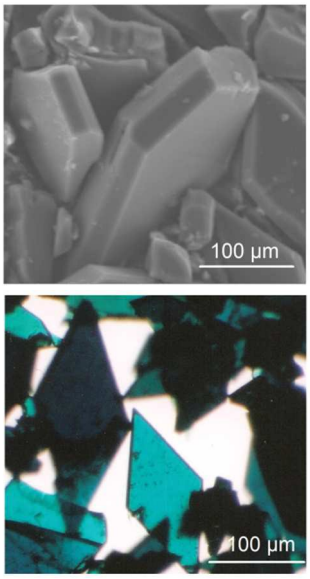

Figure 8. Crystals of **7** as viewed by scanning electron microscopy (top) and optical microscopy (bottom).

The structure of **7** was solved by SCXRD (see experimental section and Table 3) and it was shown that it corresponds to: $\{(\mathbf{6a}^{2+})_4[Fe^{II}(CN)_6]^{4-}{}_2\}\cdot 8.75H_2O$ (Fig. 9). The asymmetric unit of **7** is composed of two $[Fe^{II}(CN)_6]^{4-}$ anions, four viologen cations $\mathbf{6a}^{2+}$ and disordered water molecules. Among the viologen cations, three of them are in general positions and two $\mathbf{6a}^{2+}$ moieties are lying on crystallographic two-fold axis, thus accounting for a half unit each. Several interesting features can be highlighted with regard to the packing of the structure.

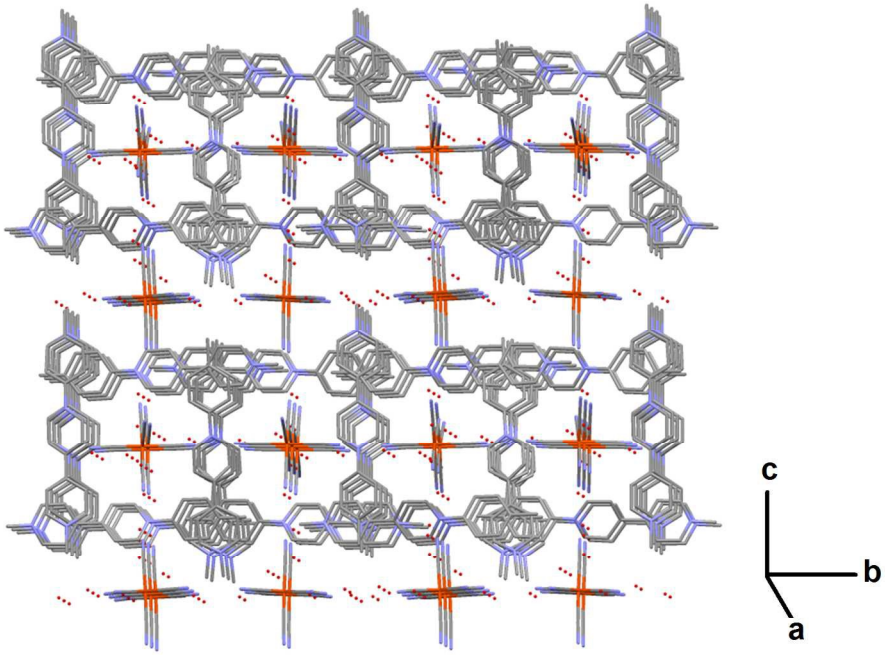

Figure 9. View of the crystal packing of **7** along a axis showing the alternance of channels of AMV **6a** cations embedding $Fe^{II}(CN)_6$ and water, and the "open" $Fe^{II}(CN)_6$ – water sheets along b. Water molecules are represented as red small spheres. Atom colors: Fe: orange; C: grey; N: blue; O: red. (All H atoms have been omitted for clarity).

The viologen cations pack in alternate orientation of 90° along crystallographic axis a (Fig. 11). They thus form successive layers of "closed tubular channels" with square section embedding ferrocyanide and water, and "open sheets" of ferrocyanide and water along crystallographic axis

b (Fig. 11). The structure of **7** also reveals the presence of hydrogen bonds, some of them being involved into a strong infinite 3-dimensional network along a, b and c of H-bonds connecting together the $Fe^{II}(CN)_6$ anions through water molecules (Fig. 11), and thus linking the "closed channels" together as well as with the "open sheet".

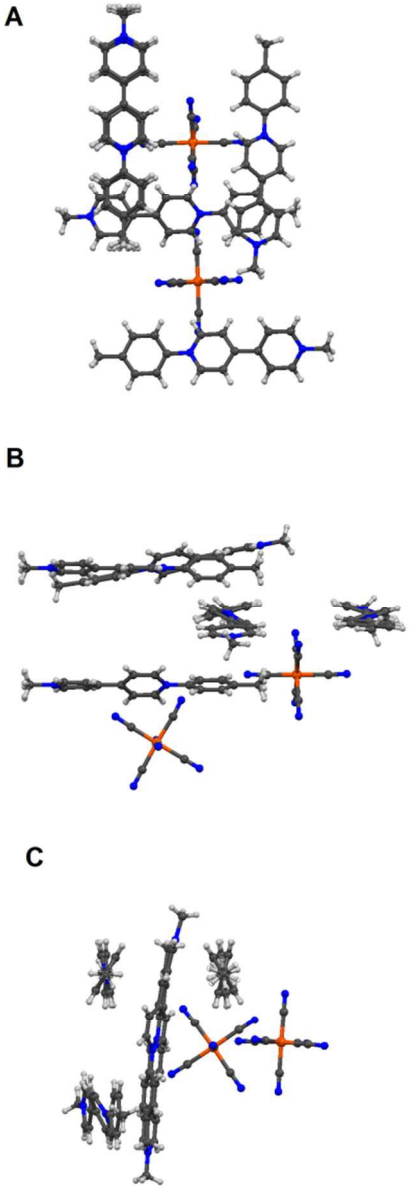

Figure 10. The crystal structure of the supramolecular complex $\{(\mathbf{6a}^{2+})_4[Fe^{II}(CN)_6]^{4-}{}_2\}\cdot 8.75H_2O$ (**7**) as viewed along the axis (A) a, (B) b and (C) c. Atom colors: Fe: orange; C: black; N: blue; H: grey. (All lattice water molecules have been omitted for clarity).

Table 3. Crystallographic data for **7**.

Formula	$C_{84}H_{89.5}Fe_2N_{20}0_{8.75}$
M_w	1630.95
Crystal system	orthorhombic
Measurement temperature/ K	293
Space group	A ea2
a/ Å b/ Å	14.6547(5) 34.5808(13)
c/ Å	35.0669(11)
V/ $Å^3$	17770.9(11)
Z	8
Dc/g.cm^{-3}	1.219
Crystal colour	green
Crystal size/mm^3	0.3*0.2*0.04
μ(Mo-Kα)/mm^{-1}	0.39
N° of refl. measured	87803
N° of unique refl.	15088
N° of observed refl.[$F^2 > 4\sigma F^2$]	11405
N° parameters refined	1107
R_1 [$F^2>4\sigma F^2$]	0.0875
wR_1 [$F^2>4\sigma F^2$]	0.2420[a]
R_2 [all refl.]	0.1107
wR_2 [all refl.]	0.2694
Goodness of fit [all refl.]	1.038
Residual Fourier/e. $Å^{-3}$	-0.942; 0.897

[a] $w=1/[\sigma^2(Fo^2)+(0.1892P)^2+10.293P]$ where $P=(Fo^2+2Fc^2)/3$

Interestingly despite the fact that the viologen moieties are not planar (the angles between their cyclic units range from 25° to 40°) their terminal aromatic rings stack parallel to each other along axis a and form an infinite network of π-π interactions: the dihedral angles between the terminal rings range from 1.8 to 8.3° and the perpendicular distances range from 3.41 to 3.69 Å. These moieties therefore build-up the edge of the closed channels.

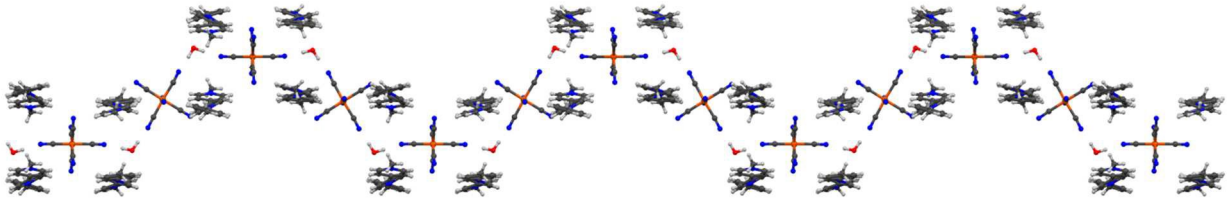

Figure 11. Infinite zigzag chain consisting of hydrogen bonded H_2O molecules and $[Fe^{II}(CN)_6]^{4-}$ anions viewed along the axis c.

Moreover, viologen / $[Fe^{II}(CN)_6]^{4-}$ clusters can be also observed. As shown in Fig. 12, four **6a**$^{2+}$ cations can enclose a $[Fe^{II}(CN)_6]^{4-}$ anion thus forming a charged cluster. Hirshfeld surface reveals the packing of a hexacyanoferrate(II) anion and the four **6a**$^{2+}$ dications in such a cluster (Fig. 12, right column).

What is interesting is that the distance between the iron center and the centroids of the pyridine rings of **6a**$^{2+}$ is not equal. The ring which is closer to Fe^{II} is the aryl substituted with a distance of 5.6-5.7 Å. The corresponding distance for the methyl substituted pyridine ring is 6.4-6.6 Å (Supplementary Information). This finding is consistent with what is observed in solution according to the ^{1}H-NMR study. In all cases of CTCs high-field shifts were greater for the *ortho*-protons of the aryl-substituted pyridine rings. In other words both in solution and in a crystal hexacyanoferrate(II) shows some preference to lie closer the substituted phenyl of the viologen,

and that is an effect caused by the non-symmetric structure of the AMVs. This is not observed in case of CTCs of symmetric viologens reported so far, and reveals the role of the viologen substitution on the charge transfer.

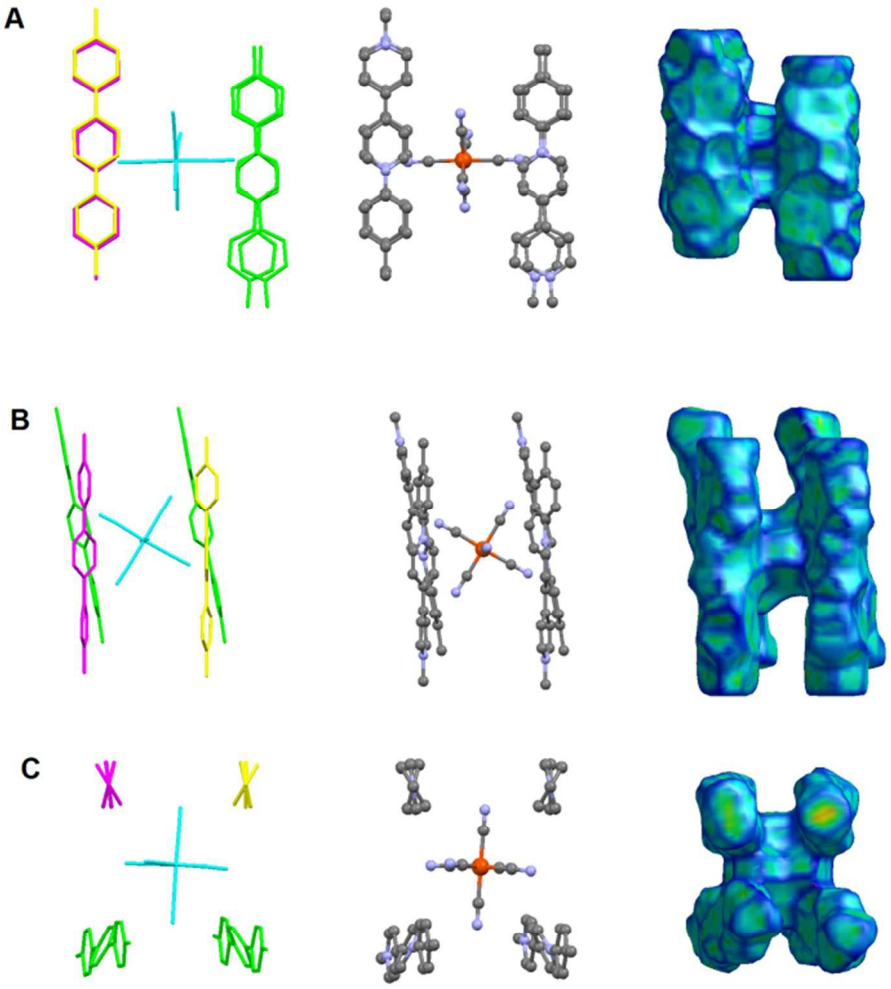

Figure 12. A hexacyanoferrate(II) anion surrounded by four viologen cations: **6a**$^{2+}$ forming a charged cluster of the type: [(**6a**)$_4$Fe^{II}(CN)$_6$]$^{4+}$ observed in the crystal structure of the CTC **7** (A) along axis a, (B) along axis b and (C) along axis c. Columns from left to right: capped stick model of the cluster with different colours indicating viologen cations of different symmetries. H atoms are omitted for clarity (left

column); ball and stick model of the cluster. H atoms are omitted for clarity (middle column); Hirshfeld surface[38] of the cluster mapped with curvedness (right column).[39,40]

Concluding remarks

The supramolecular binding of a group of synthesized aryl-methyl substituted viologens with hexacyanoferrate anions was studied in solution and in the solid state. ^{1}H-NMR studies showed that the ferrocyanide(II) anions preferentially lie closer to the aryl-substituted pyridine ring of the viologens in all cases. The structure of one of the isolated CTCs was solved and it was shown that the same trend also exists in solid crystal state. Through the determination of electron affinities of the viologen cations, it was concluded that the aryl substituent readily affects the electron withdrawing aptitude of the viologens and furthermore their propensity to form CTCs with hexacyanoferrate anions. Moreover, the linear dependence of the electron affinities of the viologen cations and the charge transfer energies is in agreement with Mulliken's theory on CTCs. Of high importance is the stabilizing role of hydrogen bonding between water molecules and hexacyanoferrates in 3-dimensional polymeric chains observed in the structure of one of the CTCs, solved through SCXRD. Such information is of high significance as it can help on better understanding solvent-ion interactions in solution.

Computational details

All calculations were performed using GAUSSIAN 09[41] program package within the DFT framework. The popular hybrid fonctionnal B3LYP[42] was employed in combination with two polarized triple-zeta split-valence basis sets from Pople 6-311G(d,p) and Ahlrichs def2-TZVP. As charge transfer processes usually involve long range interactions, we decided to employ two others functionals including dispersion effects. For that purpose, the WB97XD[43] and CAM-

B3LYP[44] were used with the same basis set as employed before. All geometry optimizations were performed with the default optimization threshold of 3×10^{-4} for the RMS Force criterion. Since all spectroscopic data were collected in water media, the Polarizable Continuum Model (PCM) was used for all calculations (ε = 78.355300). Frequency calculations were systematically carried out to ensure that the resulting structures converged to a local minimum on the potential energy surface.

Experimental Section

Physical Measurements

NMR spectra were obtained using a Varian Gemini 300 spectrometer (300 MHz ^{1}H, 75 MHz ^{13}C). Both ^{1}H and ^{13}C NMR spectra were recorded in deuterium oxide (D_2O) at 25±1 ^{o}C (compound **7** studied at 50±1 ^{o}C due to low solubility at r.t). In the case of ^{13}C NMR measurements, a few drops of [D_6]DMSO were added in solutions of the AMV chlorides in D_2O and the signal of [D_6]DMSO was used as a reference (39.39 ppm).[45] The ^{1}H NMR spectra were calibrated by using residual undeuterated solvent as an internal reference (4.79 ppm).[45] For the ^{1}H NMR spectroscopic study of CTCs, solutions containing AMV cations and hexaynoferrate anions both in concentrations of 38 mM were used. IR spectra were recorded on a Perkin Elmer Spectrum 1 FTIR spectrophotometer in the solid state (without any preparation of the samples) using the attenuated total reflectance technique (ATR) in the region 600–4000 cm^{-1}. UV–Visible spectra were recorded using a Varian CARY 1E UV–Visible spectrophotometer at 25±1 ^{o}C. The concentrations of the solutions used were 10 mM and they were prepared right before each measurement. For the UV-Vis spectroscopic study of CTCs, solutions containing AMV cations and hexaynoferrate anions both in concentrations of 10 mM were used. SEM images and EDX

analyses were obtained using a Quanta 200 FEI Scanning Electron Microscope. Single-crystal XRD analyses were performed on an Agilent SuperNova diffractometer at 293K at the MoKα radiation (λ=0.71073 Å). Data collection reduction and multiscan ABSPACK correction were performed with CrysAlisPro (Agilent Technologies). The structures were solved by direct methods with SHELXS[46] and SHELXL[46] was used for full matrix least squares refinement. All H-atoms were introduced at idealized positions and their coordinates and Uiso parameters were constraint to 1.2Ueq (parent atom) for the aromatics and 1.5Ueq (parent atoms) for the methyls and waters. Electrospray ionization (ESI) HRMS spectra were obtained on a Waters, Inc. Q-TOF Premier Mass Spectrometer (the HRMS facility of Iowa University, USA). All samples **4** and **6a-e** were dissolved in water, whereas **7** was dissolved in DMSO for the purpose of HRMS measurements. The reported m/z values correspond to the average of three repetitions per sample. The elemental analyses were performed on a Thermo Finnigan elemental analyzer EA 1112 (Spectropole, Aix-Marseille Université, Marseille, France). The results are provided with an absolute accuracy of ± 0.3% and are validated for two trials (the reported results correspond to the average of two trials in any case).

Materials and Methods

Chloro-2,4-dinitrobanzene, 4,4′-bipyridine, and the substituted anilines (**5a-e**) were purchased by ACROS Organics. Potassium ferrocyanide trihydrate and methyl iodide were purchased by FLUKA. All solvents used were purified according to literature[47] before use. Water was purified with a Barnstead EASYpure RF compact ultrapure water system and then distilled twice. Compound 1 was prepared according to a method already described in the past.[10]

Synthesis of [1-(2,4-dinitrophenyl)-1'-methyl-4,4'-bipyridine-1,1'-diium chloride iodide] (**2**)

In a 100 mL round bottom flask 1.00 g of the compound **1** (2.79 mmol) was dissolved as possible in 30 mL of absolute EtOH (with mild heating) and methyl iodide (2 mL, 32.1 mmol) was added to the resulting solution. The flask was equipped with a $CaCl_2$ tube and the solution was stirred at r.t. overnight. The precipitate was filtered off with suction, and then washed several times with absolute EtOH and diethyl ether. Finally the red solid was dried *in vacuo* for several hours. Red powder, 1.38 g (2.75 mmol) 98 %. This compound was further transformed to compound **3** by ion exchange.

Synthesis of [1-(2,4-dinitrophenyl)-1'-methyl-4,4'-bipyridine-1,1'-diium hexafluorophosphate] (**3**)

1.20 gr of the compound **2** (2.4 mmol) was dissolved in a mixture of 15 mL of H_2O and 15 mL of MeOH, with mild heating and sonication. To the warm solution an aqueous solution of NH_4PF_6 (3.60 g: 22 mmol in 5mL) was added. Immediately a shiny yellow solid precipitated. The solid was filtered off with suction and then it was washed with warm H_2O, EtOH, and finally diethylether. Finally the solid was dried for several hours under reduced pressure. Yellow powder 0.980 g (1.56 mmol) 65 %. Compound **3** was used directly for the next step without any purification.

Synthesis of [1-(2,4-dinitrophenyl)-1'-methyl-4,4'-bipyridine-1,1'-diium chloride] (**4**)

The synthesis of this compound has been reported before.[48,49] 0.980 g (1.56 mmol) of the compound **3** were easily dissolved in 6 mL of dry acetonitrile. To this solution, a solution of 4.20 g tetraethylammonium chloride (25.3 mmol) in 12 mL dry acetonitrile, was added. Immediately a yellowish precipitate was formed, which was filtered by suction, washed with dry acetonitrile and diethylether. Caution was taken during the whole procedure since compound (**4**) is

hygroscopic and forms sticky solids when exposed to moisture. The solid was dried in dessicator *in vacuo* over fresh P_2O_5 overnight. (For the needs of synthesis of **6a-e**, two batches of **4** were prepared according to the above procedure). Yellow powder, 0.590 g, 92.5%. (1.44 mmol); ^{1}H NMR (300 MHz, [D_6]DMSO): δ= 9.70 (d, *J*= 5.7 Hz, 2H; C_5H_5N), 9.35 (d, *J*= 5.1 Hz, 2H; C_5H_5N), 9.18 (s, 1H, DNPh), 9.07 (m, 3H), 8.88 (d, *J*= 5.1 Hz, 2H; C_5H_5N), 8.43 (d, *J*= 8.7 Hz, 1H; DNPh), 4.48 (s, 3H, Me); ^{13}C NMR (75 MHz, [D_6]DMSO): δ= 151.45, 149.39, 147.70, 147.21, 146.84, 143.01, 138.36, 131.96, 130.33, 126.49, 126.44, 121.55, 48.19 (Me). HRMS-ESI (m/z): $[M-2Cl^-]^+$, calcd for $C_{17}H_{14}N_4O_4$, 338.1015; found, 338.1003.

General Procedure for the synthesis of 6a-e.

0.200 g of the compound **4** (0.488 mmol) were dissolved in MeOH (5 mL). In the formed solution an excess 4:1 of the appropriate substituted aniline (**5a-e**) was added. The solution then became violet, in all cases. The solution was refluxed for a period varying from 4 to 96 h and then was cooled and 30 mL of H_2O were added. 2,4-dinitaniline was this way precipitated which was filtered, and the filtrate was condensed to dryness using a rotary evaporator. The solid was dissolved in 3 mL of MeOH and reprecipitated by adding diethyl ether, and it was collected by *in vacuo* filtration. The solids were washed with EtOH and diethyl ether, and dried *in vacuo* for several hours.

[1-(4-methylphenyl)-1'-methyl-4,4'-bipyridine-1,1'-diium chloride] (**6a**)

The synthesis of this compound has been reported before.[50] Yellow powder, 4 h reflux, 123 mg (0.369 mmol) 76 %; ^{1}H NMR (300 MHz, D_2O): δ= 9.36 (d, *J*= 6.0 Hz, 2H; C_5H_5N), 9.10 (d, *J*= 6.3 Hz, 2H; C_5H_5N), 8.71 (d, *J*= 6.3 Hz, 2H; C_5H_5N), 8.62 (d, *J*= 6.0 Hz, 2H; C_5H_5N), 7.72 (d, *J*= 7.5 Hz, 2H; Ph), 7.60 (d, J= 7.5 Hz, 2H; Ph), 4.53 (s, 3H, Me), 2.50 (s, 3H, Me-Ph); ^{13}C NMR

(75 MHz, D_2O/[D_6]DMSO): δ= 149.90, 149.11, 145.78, 144.68, 142.59, 139.34, 130.48, 126.34, 126.20, 123.18, 47.83 (Me), 19.79 (Me-Ph); UV-Vis (H_2O) $\lambda_{nm}(\log\varepsilon_{max})$: 314(3.795). HRMS-ESI (m/z): $[M-2Cl^-]^+$, calcd for $C_{18}H_{18}N_2$, 262.1470; found, 262.1461.

[1-(3-methylphenyl)-1'-methyl-4,4'-bipyridine-1,1'-diium chloride] (**6b**)

Pink colored powder, 4 h reflux, 120 mg (0.360 mmol) 74 %; ^{1}H NMR (300 MHz, D_2O): δ= 9.39 (d, *J*= 6.9 Hz, 2H; C_5H_5N), 9.13 (d, *J*= 6.6 Hz, 2H; C_5H_5N), 8.74 (d, *J*= 6.6 Hz, 2H; C_5H_5N), 8.64 (d, *J*= 6.6 Hz, 2H; C_5H_5N), 7.69 (m, 4H, Ph), 4.56 (s, 3H, Me), 2.54 (s, 3H, m-Me-Ph); 13C NMR (75 MHz, D_2O/[D_6]DMSO): δ= 149.28, 147.72, 146.82, 145.80, 142.22, 140.22, 132.12, 130.08, 126.55, 126.36, 125.16, 121.87, 47.99 (Me), 20.86 (m-Me-Ph); UV-Vis (H_2O) $\lambda_{nm}(\log\varepsilon_{max})$: 316(3.786). HRMS-ESI (m/z): $[M-2Cl^-]^+$, calcd for $C_{18}H_{18}N_2$, 262.1470; found, 262.1463.

[1-(4-fluorolphenyl)-1'-methyl-4,4'-bipyridine-1,1'-diium chloride] (**6c**)

Yellow powder, 16 h reflux, 123 mg (0.364 mmol) 75 %; ^{1}H NMR (300 MHz, D_2O): δ= 9.41 (d, *J*= 6.6 Hz, 2H; C_5H_5N), 9.14 (d, J= 5.7 Hz, 2H; C_5H_5N), 8.76 (d, *J*= 6.3 Hz, 2H; C_5H_5N), 8.65 (d, *J*= 6.3 Hz, 2H; C_5H_5N), 7.902 (m, 2H; Ph), 7.55 (m, 2H; Ph), 4.57 (s, 3H, Me); ^{13}C NMR (75 MHz, D_2O/[D_6]DMSO): δ= 152.29, 150.97, 147.84, 146.98, 128.41, 128.24, 128.08, 127.95, 119.28, 118.97, 49.86 (Me); UV-Vis (H_2O) $\lambda_{nm}(\log\varepsilon_{max})$: 316(3.812). HRMS-ESI (m/z): $[M-2Cl^-]^+$, calcd for $C_{17}H_{15}N_2F$, 266.1219; found, 266.1221.

[1-(4-bromophenyl)-1'-methyl-4,4'-bipyridine-1,1'-diium chloride] (**6d**)

Yellow powder, 24 h reflux, 133 mg (0.334 mmol) 68 %; ^{1}H NMR (300 MHz, D_2O): δ= 9.38 (d, *J*= 6.0 Hz, 2H; C_5H_5N), 9.09 (d, *J*= 5.7 Hz, 2H; C_5H_5N), 8.73 (d, *J*= 5.4 Hz, 2H; C_5H_5N), 8.61

(d, *J*= 5.1 Hz, 2H; C_5H_5N), 7.96 (d, *J*= 8.1 Hz, 2H; Ph), 7.75 (d, *J*= 7.8 Hz, 2H; Ph), 4.52 (s, 3H, Me); ^{13}C NMR (75 MHz, D_2O/[D6]DMSO): δ= 150.55, 148.84, 146.98, 145.97, 141.81, 133.84, 127.19, 127.21, 126.93, 125.82, 48.70 (Me); UV-Vis (H_2O) λ_{nm}(logεmax): 322(3.781). HRMS-ESI (m/z): $[M-2Cl^-]^+$, calcd for $C_{17}H_{15}N_2Br$, 326.0409.; found, 326.0419.

[1-(3-nitrophenyl)-1'-methyl-4,4'-bipyridine-1,1'-diium chloride] (**6e**)

Yellow powder, 96 h reflux, 125 mg (0.343 mmol) 70 %; ^{1}H NMR (300 MHz, D_2O): δ= 9.53 (d, *J*= 6.9 Hz, 2H; C_5H_5N), 9.15 (d, *J*= 6.0 Hz, 2H; C_5H_5N), 8.84 (d, *J*= 6.9 Hz, 2H; C_5H_5N), 8.72 (s, 1H, Ph), 8.68 (d, *J*= 6.6 Hz, 2H; C_5H_5N), 8.33 (d, *J*= 8.1 Hz, 1H, Ph), 8.08 (t, *J*= 8.1 Hz, ^{1}H; Ph); ^{13}C NMR (75 MHz, D_2O/[D_6]DMSO): δ= 153.32, 150.86, 150.17, 147.94, 147.20, 143.90, 133.60, 132.16, 128.71, 128.39, 128.24, 121.63, 49.95 (Me); UV-Vis (H_2O) λ_{nm}(logεmax): 313(3.698). HRMS-ESI (m/z): $[M-2Cl^-]^+$, calcd for $C_{17}H_{15}N_3O_2$, 293.1164; found, 293.1154.

Di-(1-methyl-1'-p-tolyl-4,4'-bipyridine-1,1'-diium)(hexacyanoferrate(II)) (**7**)

In an aqueous solution of **6a** (70 mg: 0.210 mmol in 400 μL H_2O), an aqueous solution of potassium ferrocyanide containing half the equimlolar quantity of $[Fe^{II}(CN)_6]\cdot 3H_2O$ (36 mg: 0.085 mmol in 400 μL H_2O) was added. The formed solution was left overnight in an open vessel resulting in a green-blue semicrystalline solid. Alternatively DMSO was added (approx. 1 mL) resulting again in a green-blue semicrystalline solid. In any case, the solid was filtered by suction and washed carefully with small quantities of H_2O, EtOH and Et_2O. Finally the solid was dried under reduced pressure. The obtained solid was purified with recrystallization from hot water (60 ^{o}C), resulting in green-blue rhombic crystals. The crystals after filtration with suction were washed with coo water, EtOH and Et_2O, and dried overnight in a high vacuum dessicator over fresh P_2O_5 until it was brought to constant weight. Green blue rhombic crystals, 105 mg

(0.064 mmol) 76 %. ^{1}H NMR (300 MHz, D_2O): δ= 9.62 (δ, *J*= 6.6 Hz, 2H; C_5H_5N), 9.40 (δ, *J*= 5.4 Hz, 2H; C_5H_5N), 9.03 (δ, *J*= 6.6 Hz, 2H; C_5H_5N), 8.94 (δ, *J*= 5.4 Hz, 2H; C_5H_5N), 8.01 (δ, *J*= 8.4 Hz, 2H; Ph), 7.88 (δ, *J*= 7.2 Hz, 2H; Ph), 4.76 (s, 3H, Me), 2.77 (s, 3H, Me_Ph); FTIR ν(C≡N):2028 cm^{-1}, ν(C=N,pyr): 1636 cm^{-1}, 1499 cm^{-1}, 1438 cm^{-1}; elemental analysis calc. for $\{(\mathbf{6a}^{2+})_2[Fe^{II}(CN)_6]^{4-}\}\cdot 8H_2O$: $C_{42}H_{52}N_{10}FeO_8$ (880.77): C, 57.27; H, 5.95; N, 15.90; found: C, 57.60; H, 5.39; N, 15.15%.

Acknowledgments

Part of this work was supported financially from the IKY foundation (Greek state scholarship foundation).

References

[1] P. M. S. Monk, *The viologens: physicochemical properties, synthesis and applications of the salts of 4,4′-Bipyridine.* John Wiley & Sons Ltd, Chichester, 1998.

[2] C. L. Bird and A. T. Kuhn, *Chem. Soc. Rev.*, 1981, **10**, 49-82.

[3] M. Möller, S. Asaftei, D. Corr, M. Ryan, and L. Walder, *Adv.Mater.*, 2004, **16**, 1558-1562.

[4] I. Deligkiozi, R. Papadakis, A. Tsolomitis, *Supramol. Chem.*, 2012, **24**, 333-343.

[5] P. Monk, R. Mortimer and D. Rosseinsky, Electrochromism and Electrochromic Devices. Cambridge University Press, Cambridge, 2007.

[6] A.L. Delacey, M.T. Bes, C. Gomezmoreno and V.M. Fernandez, *J. Electroanal. Chem.*, 1995, **390**, 69–76.

[7] Z. Sharrett, S. Gamsey, P. Levine, D. Cunningham-Bryant, B. Vilozny, A. Schiller, *et al. Tetrahedron Lett.*, 2008, **49,** 300–304.

[8] R. Papadakis, I. Deligkiozi and A. Tsolomitis, *Dyes Pigment*., 2012, **95**, 478-484.

[9] I. Deligkiozi, E. Voyiatzis, A. Tsolomitis and R. Papadakis, *Dyes Pigment*., 2015, **113**, 709-722.

[10] R. Papadakis and A. Tsolomitis, *J. Phys. Org. Chem.*, 2009, **22,** 515-521.

[11] R. Papadakis, *Chem. Phys.* 2014, **430,** 29-39.

[12] R. Papadakis and A. Tsolomitis, *J. Solut. Chem.*, 2011, **40**, 1108-1125.

[13] I. Deligkiozi, R. Papadakis and A. Tsolomitis, *Phys. Chem. Chem. Phys.* 2013, **15**, 3497-3503.

[14] J. C. Crano and R. J. Guglielmetti, editors. *Organic photochromic and thermochromics compounds. Main photochromic families*, vol. 1. Kluwer Academic Publishers, New York, 2002. pp. 341-367.

[15] K. B. Simonsen, N. Thorup, M. P. Cavac and J. Becher, *Chem. Comm.*, 1998, 901−902.

[16] A. Ponnu, J. Sung and K.G. Spears, *J. Phys. Chem. A*, 2006, **110**, 12372−12384.

[17] H. J. Hwang, S. K. Lee, S. Lee and J. W. Park, *J. Chem. Soc., Perkin Trans. 2*, 1999, 1081- 1086.

[18] A. Nakahara and J. H. Wang, *J. Phys. Chem.*, 1963, **67**, 496–498.

[19] H. E. Toma, *Can. J. Chem.*, 1979, **57**, 2079-2084.

[20] A. S. N. Murthy and A. P. Bhardwaj, *Spectrochim. Acta A*, 1982, **38**, 207-212.

[21] S. Aditya, *Spectrochim. Acta A*, 1988, **44**, 941-942.

[22] V.-S. Eller, M. Adam and R. D. Fischer, *Angew. Chem.*, 1990, **102**, 1157-1159.

[23] S. A. Kostina, A. B. Ilyukhin, B. V. Lokshin and V. Y. Kotov, *Mendeleev Commun.*, 2001, **11**, 12–13

[24] A. S. Abouelwafa, V. Mereacre, T. S. Balaban, C. E. Anson and A. K. Powell, *Cryst. Eng. Commun.*, 2010, **12**, 94–99.

[25] W. S. Hammack, H. G. Drickamer and D. N. Hendrickson, *Chem. Phys. Lett.*, 1988, **151**, 469-473.

[26] T. Kinuta, T. Sato, N. Tajima, R. Kuroda, Y. Matsubara and Y. Imai, *J. Mol. Struct.*, 2010, **982**, 45–49.

[27] M. Nanasawa, M. Kaneko and H. Kamogawa, *Bull. Chem. Soc. Jpn.*, 1993, **66**, 1764-1767.

[28] V. Y. Kotov, A. B. Ilyukhin and A. V. Zenin, *Russ. J. Inorg. Chem.*, 2008, **53**, 552-556.

[29] M. Hofbauer, M. Möbius, F. Knoch, R. Benedix, *Inorg. Chim. Acta*, 1996, **247**, 147−154.

[30] R. S. Mulliken, *J. Am. Chem. Soc.*, 1952, **14**, 811-824.

[31] C. J. Bender, *Chem. Soc. Rev.*, 1986, **15**, 475-502.

[32] A. C. Benniston, A. Harriman, P. Li., J. P. Rostron, R. W. Harrington and W. Clegg, *Chem. Eur. J.*, 2007, **13**, 7838-7851.

[33] R. Haque , W. R. Coshow and Le-R. F. Johnson, *J. Am. Chem. Soc.*, 1969, **91**, 3822–3827.

[34] P. M.S. Monk, N. M. Hodgkinson and R. D. Partridge, *Dyes Pigment.*, 1999, **43**, 241-251.

[35] B. G.White, *Trans. Faraday Soc.*, 1969, **65**, 2000-2015.

[36] G. Saielli, *J. Phys. Chem. A* 2008, **112**, 7987-7995.

[37] Similar correlations have been observed by Hofbauer *et al.* for diquats through the NDDO formalism.[29]

[38] M. A. Spackman and D. Jayatilaka, *Cryst. Eng. Commun.*, 2009, **11**, 19-32.

[39] Visualized using GDIS Molecule Modeller.[40]

[40] S. Fleming and A. Rohl, *Z. Kristallogr.* 2005, **220**, 580−584.

[41] Gaussian 09, Revision D.01, M. J. Frisch, G. W. Trucks, H. B. Schlegel, G. E. Scuseria, M. A. Robb, J. R. Cheeseman, G. Scalmani, V. Barone, B. Mennucci, G. A. Petersson, H. Nakatsuji, M. Caricato, X. Li, H. P. Hratchian, A. F. Izmaylov, J. Bloino, G. Zheng, J. L. Sonnenberg, M. Hada, M. Ehara, K. Toyota,

R. Fukuda, J. Hasegawa, M. Ishida, T. Nakajima, Y. Honda, O. Kitao, H. Nakai, T. Vreven, J. A. Montgomery, Jr., J. E. Peralta, F. Ogliaro, M. Bearpark, J. J. Heyd, E. Brothers, K. N. Kudin, V. N. Staroverov, T. Keith, R. Kobayashi, J. Normand, K. Raghavachari, A. Rendell, J. C. Burant, S. S. Iyengar, J. Tomasi, M. Cossi, N. Rega, J. M. Millam, M. Klene, J. E. Knox, J. B. Cross, V. Bakken, C. Adamo, J. Jaramillo, R. Gomperts, R. E. Stratmann, O. Yazyev, A. J. Austin, R. Cammi, C. Pomelli, J. W. Ochterski, R. L. Martin, K. Morokuma, V. G. Zakrzewski, G. A. Voth, P. Salvador, J. J. Dannenberg, S. Dapprich, A. D. Daniels, O. Farkas, J. B. Foresman, J. V. Ortiz, J. Cioslowski, and D. J. Fox, Gaussian, Inc., Wallingford CT, 2013.

[42] A.D. Becke, *J. Chem. Phys.* 1993, **98**, 5648.

[43] J.-D. Chai and M. Head-Gordon, *Phys. Chem. Chem. Phys.*, 2008, **10**, 6615-6620.

[44] T. Yanai, D. Tew and N. Handy, *Chem. Phys. Lett.*, 2004, **393**, 51-57.

[45] H. E. Gottlieb, V. Kotlyar and A. Nudelman, *J. Org. Chem.*, 1997, **62**, 7512–7515.

[46] G. M. Sheldrick, *Acta Cryst. A*, 2008, **64**, 112-122.

[47] D. D. Perrin and L. F. Armarego, *Purification of laboratory chemicals*. Pergamon, Exeter, 1988.

[48] V.-A. Constantin, L. Cao, S. Sadaf and L. Walder, *Phys. Status Solidi B*, 2012, **249**, 2395–2398.

[49] T. Mochida, Y. Funasako, Y. Nezu, K. Hagiwara and R. Horikoshi, *Eur. J. Inorg. Chem.* 2015, 2330–2337.

[50] M. Freitag and E. Galoppini, *Langmuir* 2010, **26**, 8262–8269.

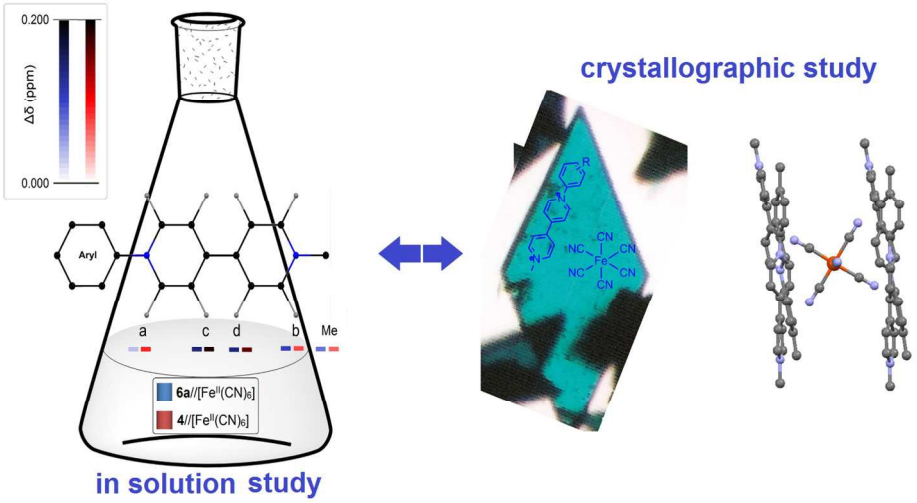

400x200mm (120 x 120 DPI)